Critical and paramagnetic spin dynamics in an antiferromagnetically coupled Heisenberg magnet: results for RbMnF$_3$

Critical and paramagnetic spin dynamics in an antiferromagnetically coupled Heisenberg magnet: results for RbMnF₃

A Cuccoli†, S W Lovesey‡ and V Tognetti†

† Department of Physics, University of Florence, L E Fermi 2, I-50125, Italy
‡ DRAL Rutherford Appleton Laboratory, Oxfordshire OX11 0QX, UK

Abstract. Results are provided for the spin–spin response function of a three-dimensional, antiferromagnetically coupled Heisenberg magnet covering a range of temperatures from the critical temperature to deep in the paramagnetic phase. The wave vectors considered span the Brillouin zone. Damping rates are given at the zone centre and the antiferromagnetic-ordering wave vector, w, together with copious numerical results for the full response function. The calculations are based on the non-linear, integral–differential equations obtained from so-called coupled-mode theory. In a confrontation between experimental and theoretical findings for RbMnF₃ nearly all aspects have a positive outcome. The main exception is found at T_c for wave vectors close to w. Here, the measured response comprises three distinct components, reasonably ascribed to diffusive and oscillatory collective processes. In the corresponding predictions, the diffusive component is conspicuously missing. A less pronounced discrepancy if found at the antiferromagnetic zone boundary where, once again, there is more structure in the observed spectrum than in the calculated one.

1. Introduction

Over the past few decades, studies of the time-dependent properties of spin systems have played a significant role in the development of the current sophisticated theory of dynamical processes in condensed matter. Up to the end of the 1960s, theoretical methods for spin systems tended to depend on the use of frequency moments, following very early ideas from Van Vleck and De Gennes, among others (for a review of this work see, for example, Marshall and Lowde 1968). These methods are not reliable at the critical temperature, where an infinite number of degrees of freedom are responsible for non-trivial features in the dynamics. Seminal work on this aspect of spin dynamics was reported by Wegner (1969), Résibois and DeLeener (1969) and Kawasaki (1970). It is now recognized, largely through the work of Hubbard (1971), that these developments all lead to the same system of closed non-linear equations for the time-dependent and wave-vector-dependent spin–spin response function. Today, the equations are often referred to as the coupled-mode theory of the dynamical properties of spin systems.

Appropriate variants of coupled-mode theory have been successfully used to investigate properties of other highly correlated systems. Notable examples are models of the glass transition, and localization in the Anderson model. It is interesting to note in studies of fluids a strong similarity between the coupled-mode theory for fluctuations close to equilibrium and the direct-interaction theory of turbulence when the need for separate equations for the

response and propagator are relaxed, i.e. the theory is reduced to the description of small fluctuations close to thermal equilibrium.

Applied to critical spin dynamics, coupled-mode theory is in accord with two other powerful approaches. One, scaling theory, is a set of postulates that lead to predictions in the critical region from a knowledge of various properties in the hydrodynamical region. The renormalization-group method provides asymptotic properties of the spin-correlation function and explicit results for some critical exponents. Even though this method does not provide closed equations for the spin-response function, it is particularly valuable since it alone is a systematic, perturbative approach to critical phenomena in spin systems, and other models which display a continuous phase transition. Results derived for spin systems using dynamic-scaling arguments and the renormalization-group method are gathered, together with copious references, by Privman *et al* (1990).

Although the pioneers of the coupled-mode approach concentrated attention on the critical properties of spin systems, there is a body of evidence to the effect that it provides an unrivalled account of paramagnetic fluctuations of short and long wavelengths (Hubbard 1971, Cuccoli *et al* 1989, 1990, Westhead *et al* 1991). Perhaps the most recent example of the reliability of coupled-mode theory outside the critical region is in its application to a spin chain at infinite temperature (Lovesey and Balcar 1994). In this case, the theory provides insight to non-hydrodynamical behaviour observed in data from extensive computer simulations (Srivastava *et al* 1994).

In this paper we continue the investigation of coupled-mode theory applied to spin systems by providing the first comprehensive study of an antiferromagnetically coupled Heisenberg magnet. Previous work on this system has focused on the critical and hydrodynamic limits (Wegner 1969, Huber and Krueger 1970, Bagnuls and Joukoff-Piette 1975). Here, we survey the spin–spin response function at the critical temperature, T_c, for all wave vectors in the Brillouin zone. In particular, at T_c we predict the behaviour of the van Hove response function, $S(k, \omega)$, for the three special wave vectors, k; near the chemical zone centre, the antiferromagnetic zone boundary, at which in the condensed phase the linear spin-wave dispersion achieves its maximum value, and the antiferromagnetic ordering wave vector, w. Above T_c, we show, starting deep in the paramagnetic phase and approaching T_c, how developing antiferromagnetic correlations manifest themselves in the time-dependent spin fluctuations. A combination of numerical and analytical methods of analysis are employed; the latter is used to demonstrate that, for the antiferromagnetically coupled system, coupled-mode theory is consistent with results derived with dynamic-scaling arguments and the renormalization-group method.

Where possible, theoretical results are compared with experimental data for $S(k, \omega)$ obtained on $RbMnF_3$, using inelastic neutron scattering, by Tucciarone *et al* (1971a, b). By and large, agreement between experimental and theoretical results is strikingly good. However, at T_c and for k in the vicinity of the antiferromagnetic ordering wave there is an obvious disagreement: the experimental data for $S(k, \omega)$ shows a three-peaked structure, namely, a central ($\omega = 0$) diffusive mode and two side peaks attributed to collective spin oscillations, albeit heavily damped oscillations, while theoretical results for the appropriate wave vectors show only two collective mode peaks. The latter feature is consistent with results reported by Wegner (1969), independently confirmed by Hubbard (1972 private communication). Here, we provide a more extensive picture of the disagreement between experimental and theoretical data. Since, to the best of our knowledge, this is the only example of its kind there is a case for new experiments; progress over the past two decades with neutron sources, instrumentation, and data analysis methods probably mean that data

for $S(k, \omega)$ obtained by Tucciarone *et al* (1971a, b) can be improved on (exceptional-quality data can be obtained at $k \sim w$ because there is next-to-no nuclear Bragg scattering contaminating the magnetic signal).

The next two sections describe the Heisenberg spin model and the corresponding coupled-mode theory (a detailed derivation of the theory and some of its properties is provided by Lovesey 1986 and Cuccoli *et al* 1989). Decay rates near T_c, for the critical and hydrodynamical regions, are derived in section 4. the findings demonstrate that coupled-mode theory is consistent with dynamic-scaling arguments, and provide useful insight into the numerical results given in the subsequent two sections.

2. Model

Spin operators S_a are placed on a lattice with N sites labelled by the index a. The spins interact through a Heisenberg interaction of strength J, so the model Hamiltonian is

$$\mathcal{H} = J \sum_{a,b} S_a \cdot S_b \tag{2.1}$$

where the sum is over all nearest-neighbour pairs on the lattice.

We will study the time development of spatial Fourier components $S(k)$ defined through

$$S_a = (1/N) \sum_k \exp(-\mathrm{i}k \cdot R_a) S(k). \tag{2.2}$$

The isothermal susceptibility is

$$\chi(k) = \tfrac{1}{3}(S(k), \cdot S(-k)). \tag{2.3}$$

Here, (,) denotes a Kubo relaxation function; for classical variables $(A, B) = (\langle AB \rangle / T)$ where the angular brackets denote a thermal average, and T is the temperature ($k_B = \hbar = 1$). The dynamical properties of (2.1) are studied in terms of the normalized relaxation function,

$$F(k, t) = \tfrac{1}{3}(S(k, t), \cdot S(k))/\chi(k) \tag{2.4}$$

where $S(k, t)$ is the standard Heisenberg time-dependent operator. The spectrum of neutrons inelastically scattered by spin fluctuations is proportional to

$$S(k, \omega) = (1/2\pi) \int_{-\infty}^{\infty} \mathrm{d}t \exp(-\mathrm{i}\omega t) F(k, t). \tag{2.5}$$

In the context of neutron scattering, ω is the energy transferred from the primary beam to the spin fluctuations. The concomitant change in the wave vector of the neutrons is $k = w + q$, where w is an antiferromagnetic-ordering wave vector.

3. Coupled-mode theory

In view of the fact that coupled-mode theory for spin systems has recently been reviewed, we will provide in this section no more material beyond that required to define notation.

Coupled-mode theory is a closed set of equations for $F(k, t)$. The latter is determined by

$$\partial_t F(k, t) = -\int_0^t dt' F(k, t - t')K(k, t') \tag{3.1}$$

and the so-called memory function, $K(k, t)$, is approximated by

$$K(k, t) = (2T/\chi(k))\sum_p \{\gamma_{p-k} - \gamma_p\} F(p, t)F(p - k, t)/(\mu_0 + \gamma_p). \tag{3.2}$$

Here γ_k is a geometric factor that depends on the point group symmetry of the lattice; for a simple cubic lattice with a cell length a_0

$$\gamma_k = \tfrac{1}{3}(\cos(a_0 k_x) + \cos(a_0 k_y) + \cos(a_0 k_z)) = 1 - \rho^2 k^2 + \dots.$$

The quantity μ_0 varies with temperature. In fact, the temperature scale is determined by the spherical model of spin correlations, namely

$$(2rJS(S + 1)/3T) = (1/N)\sum_p (\mu_0 - \gamma_p)^{-1} = I(\mu_0) \tag{3.3}$$

in which r is the number of nearest neighbours ($r = 6$, SC), and the integral on the right-hand side is the standard extended Watson integral.

For a simple cubic lattice, the critical temperature, T_c, satisfies

$$4JS(S + 1)/T_c = 1.5164. \tag{3.4}$$

The spherical model susceptibility is

$$\chi(k) = \{N/2rJ(\mu_0 + \gamma_k)\}. \tag{3.5}$$

In the key equations (3.1), (3.2) and (3.5) the wave-vector variables p and k are general wave vectors in the Brillouin zone for the reciprocal lattice of the chemical structure.

As the critical temperature is approached from above, $\mu_0 \rightarrow 1$, and the susceptibility has a maximum at the antiferromagnetic-ordering wave vector, w, for which $\gamma_w = -1$. Hence, for $(\mu_0 - 1) \ll 1$ we expand the geometric factor γ_k in the susceptibility about w using the small-argument expansion, and find an Ornstein–Zernike form

$$\chi(k) = \{N/2rJ\rho^2(\kappa^2 + q^2)\} \tag{3.6}$$

in which the inverse correlation length, κ, satisfies

$$\rho^2 \kappa^2 = (\mu_0 - 1) \tag{3.7}$$

and q is measured relative to w. For the spherical model, (3.7) leads to $\kappa \sim (T - T_c)^\nu$ where the critical exponent $\nu = 1$.

4. Decay rates

For temperatures very close to T_c, such that $\rho\kappa \ll 1$, and very small wave vectors, the spin relaxation function $F(k, t)$ is expected to approach an exponential function of time for sufficiently long times. The associated decay rates can be estimated from equation (3.2) for the memory function.

To this end, in (3.2) we shift the wave vector p in the summation by an amount w, and use the identity $\gamma_{p+w} = -\gamma_p$. One finds

$$K(k, t) = \left(2T_c/\chi(k)\right) \sum_p \{\gamma_p - \gamma_{k-p}\} F(p+w, t) F(k-w-p, t)/\left(\mu_0 - \gamma_p\right). \tag{4.1}$$

In the limit $(\mu_0 - 1) \ll 1$, the denominator in the kernel emphasizes the region where $\rho p \ll 1$, so it is appropriate to expand all functions in p. If the decay rates near $k = 0$ and $k = w$ are denoted by Γ_0 and Γ, respectively, we obtain from (4.1) evaluated in the limit $k \to 0$,

$$\Gamma(k) = (A/2)k^2 \int_k p^2 \mathrm{d}p / \{\Gamma(p)(\kappa^2 + p^2)\}. \tag{4.2}$$

Here, the (non-universal) material constant

$$A = \left(4T_c r J v_0/\pi^2\right) \tag{4.3}$$

where v_0 is the volume of the chemical unit cell. It is prudent to express the decay rates in terms of a dimensionless parameter $\theta = (k/\kappa)$; let

$$\Gamma_0 = k^2 (A/\kappa)^{1/2} h_0(\theta)$$

and, near the ordering vector where $\theta = (q/\kappa)$,

$$\Gamma(q) = \kappa^{3/2}\left(1 + \theta^2\right) A^{1/2} h(\theta). \tag{4.4}$$

From (4.2) we obtain the following integral equations for the dimensionless functions $h(\theta)$ and $h_0(\theta)$:

$$h_0(\theta) = \tfrac{1}{2} \int_\theta \zeta^2 \mathrm{d}\zeta / \{(1 + \zeta^2)^2 h(\zeta)\}. \tag{4.5}$$

If we apply (4.1) to the case where k is in the vicinity of w, i.e. $q \to 0$,

$$h(\theta) = \int_\theta \zeta^2 \mathrm{d}\zeta / \{(1 + \zeta^2)[(1 + \zeta^2)h(\zeta) + \zeta^2 h_0(\zeta)]\}. \tag{4.6}$$

The pair of equations (4.5) and (4.6) determine the functions $h_0(\theta)$ and $h(\theta)$.

In the critical limit, $\theta \to \infty$,

$$\Gamma_0(q) = \Gamma(q) = q^{3/2} A^{1/2}. \tag{4.7}$$

From this result it follows that the dynamic critical exponent $z = \tfrac{3}{2}$. In the opposite, hydrodynamical limit, $\theta \to 0$, and it can be shown that $h_0(\theta)$ and $h(\theta)$ tend to constant values determined by (4.5) and (4.6) evaluated with $\theta = 0$;

$$\Gamma_0(k) = 0.553 k^2 (A/\kappa)^{1/2} \tag{4.8}$$

and

$$\Gamma(q) = 0.711 A^{1/2} \kappa^{3/2}\left(1 + (q/\kappa)^2\right).$$

Hence, $\Gamma(0)$ decreases as the critical temperature is approached with a power-law behaviour $(T - T_c)^{z\nu}$. On the other hand, $\Gamma_0(k)$ increases with decreasing temperature with a power law $(T - T_c)^{-\nu/2}$. The decrease of $\Gamma(0)$ as T approaches T_c is expected since w is a Bragg position for the magnetic condensate.

5. Numerical results

The numerical method for the solution of the coupled equations (3.1) and (3.2) is described by Cuccoli *et al* (1989). Here, we provide results for the response function (2.5) for several different temperatures. All the results are for a nearest-neighbour exchange model, defined by (2.1), in which the spins are arranged on a simple cubic lattice with a cell length a_0.
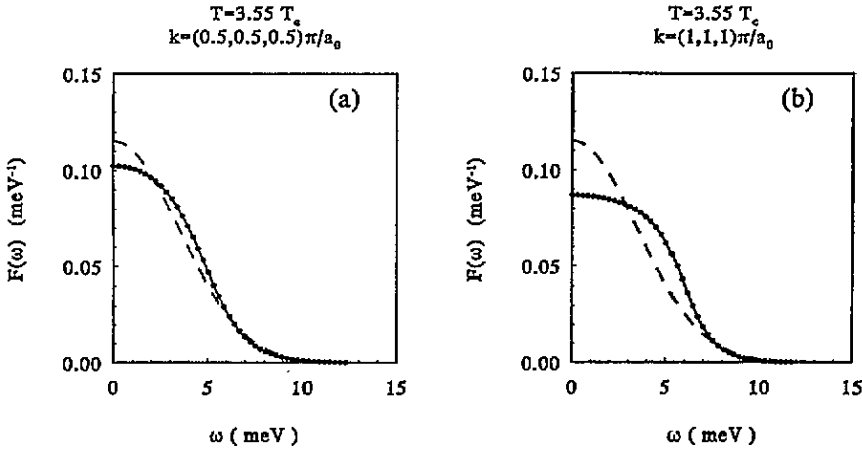

Figure 1. $S(k, \omega)$ is displayed for two values of k as a function of ω. The wave vectors, measured in units of (π/a_0), correspond to the antiferromagnetic zone boundary, $k = (\frac{1}{2}, \frac{1}{2}, \frac{1}{2})$, and the antiferromagnetic-ordering wave vector, $k = w = (1, 1, 1)$. The temperature $T = 3.55 T_c$. Included in the figures is a Gaussian function whose mean square width is calculated from the second-frequency moment evaluated for the spherical model, see (5.1) and (5.2). The exchange parameter $J = 0.29$ meV, and the spin $S = \frac{5}{2}$.

At high temperatures, physical intuition leads one to expect that spin correlations will be strongest at quite short distances, probed by large wave vectors. This expectation is borne out by the results for $T = 3.55 T_c$ shown in figure 1. In order to assess the influence of the correlations on $S(k, \omega)$ for $k = (\frac{1}{2}, \frac{1}{2}, \frac{1}{2})$ and $k = (1, 1, 1) = w$, measured in units of (π/a_0), we have included in figure 1 the function

$$\left(2\pi\omega_0^2\right)^{-1/2} \exp\left(-\omega^2/2\omega_0^2\right) \tag{5.1}$$

in which ω_0^2 is the second frequency moment evaluated with the spherical model of static spin correlations, namely

$$\omega_0^2(k) = \tfrac{8}{3}\left(rJ\mu_0\right)^2 S(S+1)\left(1 - \gamma_k\right)\left(1 + \gamma_k/\mu_0\right)\left\{1 - 1/\mu_0 I\left(\mu_0\right)\right\} \tag{5.2}$$

and $I(\mu_0)$ is defined in (3.3). The departures of $S(k, \omega)$ from the Gaussian function are, indeed, most significant at the largest k.

Antiferromagnetic correlations are not apparent in the results for $T = 3.55 T_c$ inasmuch that departures from a Gaussian are more pronounced at w than at the antiferromagnetic zone boundary $(\frac{1}{2}, \frac{1}{2}, \frac{1}{2})$. At the lower temperature $T = 1.25 T_c$ this is no longer the case. Figure 2 shows that at this temperature there is structure in $S(k, \omega)$ for $k = (\frac{1}{2}, \frac{1}{2}, \frac{1}{2})$ not present at $k = w$. To illustrate the antiferromagnetic character of the structure obtained at
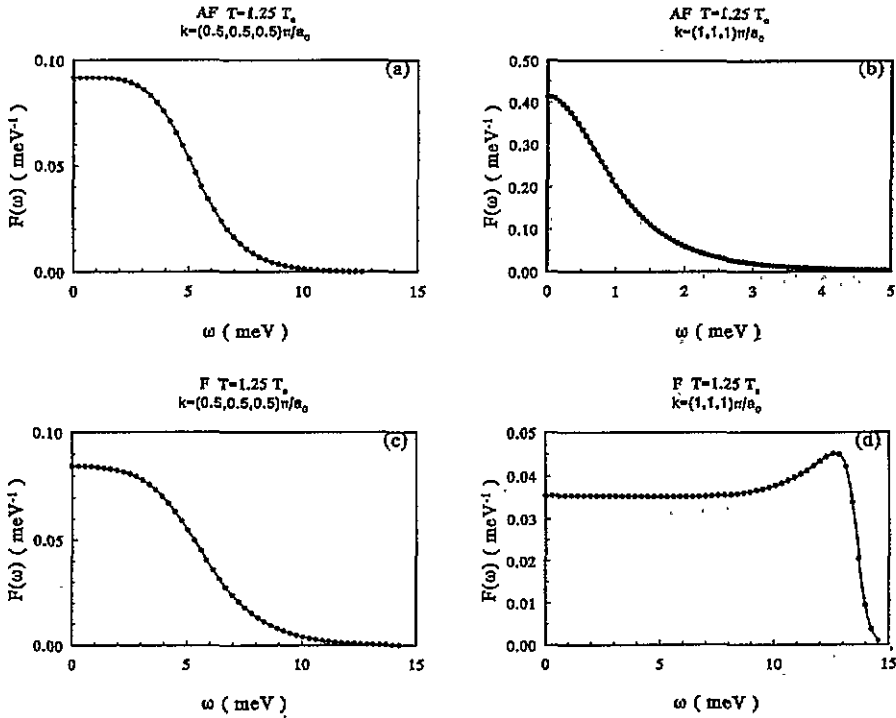
Figure 2. $S(k, \omega)$ is shown for $T = 1.25T_c$ and ferromagnetic (F) and antiferromagnetic (AF) coupling. Note that $k = w$ is the ferromagnetic zone boundary. Parameters used, apart from the sign of J, are the same as in figure 1.

$k = (\frac{1}{2}, \frac{1}{2}, \frac{1}{2})$, we have included the corresponding results for a ferromagnetically coupled system ($J \to -J$ in (2.1)). For this case the ferromagnetic spin correlations probed at the ferromagnet zone boundary $k = (1, 1, 1)$, support a collective oscillation with a relatively long lifetime. The changes in energy scales for $S(k, \omega)$ seen in figure 2 for different k and different exchange couplings can be understood from the behaviour of the second frequency moment (5.2); for a ferromagnetic exchange $(1 + \gamma_k/\mu_0) \to (1 - \gamma_k/\mu_0)$, while all other factors remain the same, and $\mu_0 \sim 1$ near T_c. It is interesting to note that on setting $\mu_0 = 1$ one finds $\omega_0^2 \propto \varepsilon_k^2$, where ε_k is the linear spin-wave spectrum. For ferromagnetic (antiferromagnetic) coupling ε_k is a maximum at the zone boundary $k = w(k = (\frac{1}{2}, \frac{1}{2}, \frac{1}{2}))$. Hence, the relatively narrow spectrum at $k = w$ for an antiferromagnetic exchange coupling can be viewed as a signature of incipient antiferromagnetic ordering.

Lastly, we turn to results for $T = T_c$. Figure 3 shows $S(k, \omega)$ with k close to the zone centre and near w. The antiferromagnetic correlations near w produce a peak at a non-zero frequency, which gradually becomes less of a feature with increasing $q = k - w$. The significant differences in $S(k, \omega)$ at $k \sim 0$ and $k \sim w$ have been predicted by Wegner (1969). The widths of the spectra shown in figure 3 are consistent with the $q^{3/2}$ scaling demonstrated in section 4. Figure 4 illustrates that at T_c there are no special features in the response function at the antiferromagnetic zone boundary, and the width of the spectrum is consistent with the estimate derived from (5.2).
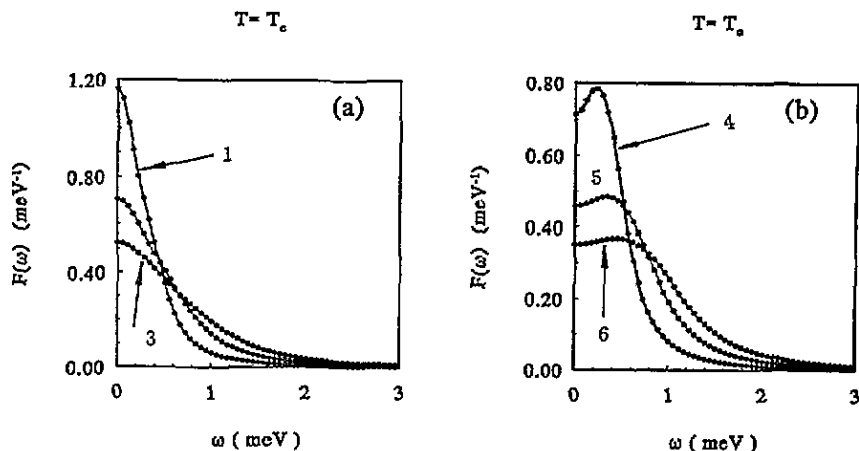
Figure 3. $S(k, \omega)$ is displayed for $T = T_c$, and k close to the Brillouin zone centre and the antiferromagnetic-ordering wave vector $w = (1, 1, 1)$. The wave vectors in units of $(\pi/12a_0)$ are 1, (0,0,1); 2, (0,1,1); 3, (1,1,1); 4, (11,12,12); 5, (11,11,12) and 6, (11,11,11). Other parameters are the same as those used in figure 1.
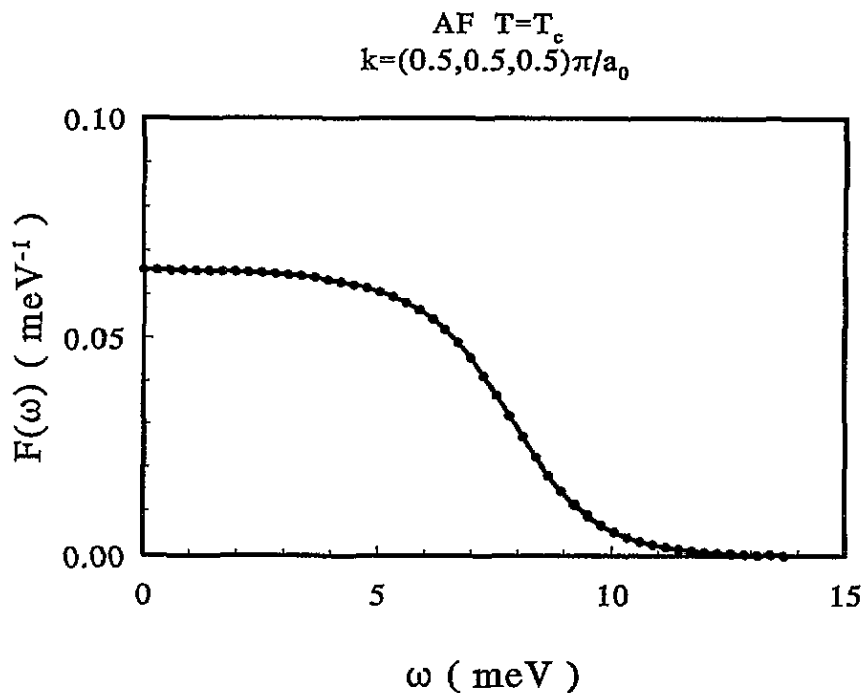

Figure 4. The van Hove response function $S(k, \omega)$ is shown for $T = T_c$, and $k = (\frac{1}{2}, \frac{1}{2}, \frac{1}{2})$, which is the antiferromagnetic zone boundary where the corresponding second frequency moment, used to calculate the Gaussian approximation to $S(k, \omega)$, achieves its maximum value in the Brillouin zone.

6. Comparison with experimental data

Experimental studies of time-dependent spin fluctuations in magnetic systems that focus on critical phenomena are reviewed by Cowley (1987) and Collins (1989). Of the many materials included in these reviews, our attention is directed to the perovskite crystal $RbMnF_3$, which is an excellent example of a simple isotropic antiferromagnetic salt. Indeed, the Hamiltonian for $RbMnF_3$ is probably closer to that of an ideal model that is that of any other magnetic system (Collins 1989).

Table 1. Properties of $RbMnF_3$.

Quantity	Symbol	Value
Chemical unit-cell dimension	a_0	4.24 Å
Critical temperature[a]	T_c	83 K
Nearest neighbour exchange interaction	J	0.29 meV
Non-universal material constant in the damping rate	A	361.1 meV^2 Å^3
Superlattice wave vector	w	(π/a_0) (1, 1, 1)
Geometrical factor ($\alpha = x, y, z$)	γ_k	$\frac{1}{3}\sum_\alpha \cos(a_0 k_\alpha)$
Number of nearest neighbours	r	6
Spin magnitude	S	5/2

[a] The quoted value of J and the spherical-model relation (3.4) produce a critical temperature of 78 K. Windsor and Stevenson (1966) report the value $J = 0.29 \pm 0.03$ meV obtained from an analysis of the spin-wave dispersion. All our results are provided as a function of the reduced temperature (T/T_c), and A is calculated with $T_c = 78$ K.

Various properties of $RbMnF_3$ are gathered in table 1. The Mn ions are arranged on a simple cubic lattice, and the spin magnetic moments order antiferromagnetically below T_c with the moments directed along the sides of the magnetic unit cells. The experimental studies performed by Windsor and Stevenson (1966) show that the dominant exchange interactions are between nearest-neighbour ions, and there is next-to-no magnetic anisotropy. In consequence, the magnetic properties of $RbMnF_3$ are believed to be described by the Heisenberg Hamiltonian (2.1), to a very good approximation.

In the development of magnetic neutron scattering, an early detailed study of dynamic spin fluctuations in critical and paramagnetic regions was performed by Tucciarone *et al* (1971a, b) on $RbMnF_3$. We will review and contrast their findings at T_c and in the paramagnetic phase in the context of our findings for coupled-mode theory applied to the Heisenberg model (2.1). In our formulation of the coupled-mode theory we have set $\eta = 0$. Additionally, we have chosen to use the experimentally determined value of J, rather than opt for a value such that the spherical-model T_c agrees with the observed value, cf. table 1.

At $T = T_c$, the width of the response function near the antiferromagnetic Bragg peak is found experimentally to vary with the wave vector as q^z at small q, and $z = 1.4 \pm 0.1$. Above the critical temperature, antiferromagnetic Bragg reflections cease to exist as the lattice symmetry changes so as to make all sites equivalent. This means that there is no reason for the decay rate to go to zero as the wave vector q, measured relative to w goes to zero. The experiments show a dynamic response that is approximately of Lorentzian form at $q = 0$. The observed width varies with temperature according to a critical exponent of $(1.46 \pm 0.13)\nu$, whereas the coupled-mode theory, reported in section 4, predicts an exponent of $z\nu$ such that $z = 1.46 \pm 0.13$, as shown in table 2. This value is in satisfactory agreement with the prediction $z = \frac{3}{2}$, and the experimental result obtained at $T = T_c$.

Table 2. A comparison of critical exponents of RbMnF$_3$ as measured by Tucciarone *et al* (1971a, b) with predictions for the isotropic Heisenberg model (after Collins 1989).

Exponent	Experiment	Calculation
γ	1.366±0.024	1.388±0.003
ν	0.701±0.011	0.707±0.003
η	0.055±0.010	0.037±0.009
z^{a}	1.46±0.13	1.5

[a] The value for the dynamic critical exponent, $z = \frac{3}{2}$ is obtained from the coupled-mode equation, section 4, and also dynamic-scaling arguments and renormalization-group calculations.
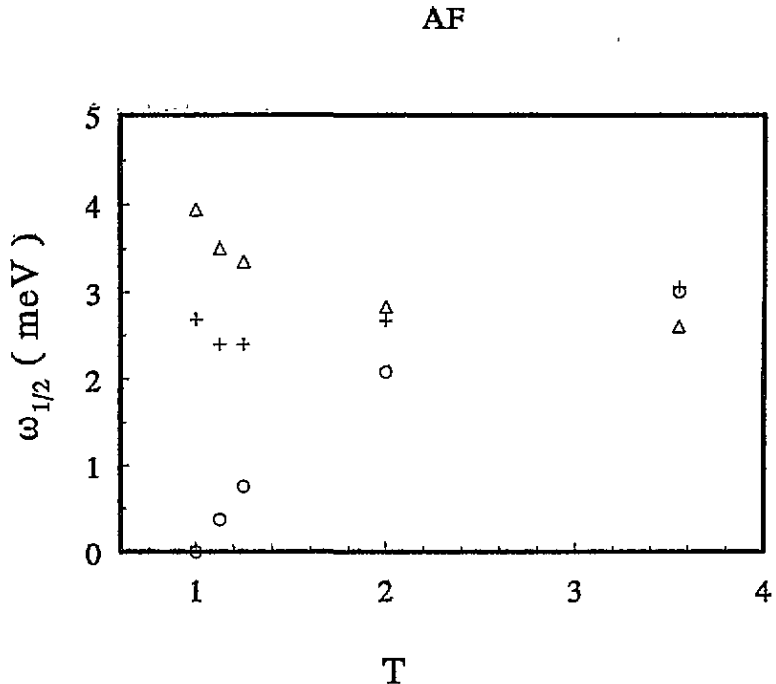
AF

Figure 5. Widths at half area of $S(k, \omega)$, examples of which are shown in figures 1, 2 and 4, are given at three wave vectors and five reduced temperatures. The three wave vectors are $k = w$ (O), $k = (\frac{3}{4}, \frac{3}{4}, \frac{3}{4})$ (+) and $(\frac{1}{2}, \frac{1}{2}, \frac{1}{2})$ ($\triangle$). Wave vectors are measured in units of (π/a_0) where a_0 is the length of a side of the (cubic) chemical unit cell. When comparing these results with the corresponding experimental data for RbMnF$_3$ reported by Tucciarone *et al* (1971a) bear in mind that these authors quote wave vectors in units of $(2\pi/a_0)$.

Turning to the results of our coupled-mode theory, figure 5 shows the half areas of $S(k, \omega)$ for three values of k and five values of (T/T_c). Theoretical and experimental results (Tucciarone *et al* 1971a) are in good agreement on an absolute basis. Note that the half area at $k = w$ decreases as T approaches T_c, while at the antiferromagnetic zone boundary $k = (\frac{1}{2}, \frac{1}{2}, \frac{1}{2})$ it increases with decreasing T. This behaviour is in accord with the predicted decay rates (for a Lorentzian response function the decay rate and half area are the same). At T_c, we predict $\Gamma(q) = q^{3/2}A^{1/2}$ for $\rho q \ll 1$, and the material parameters for RbMnF$_3$ give the value $A^{1/2} = 19.0$ meV Å$^{3/2}$, whereas the observed half area of the response function for $\rho q \ll 1$ scales as $q^{3/2}$, as already noted, and the constant

of proportionality is 16.0 meV $\text{Å}^{3/2}$. This tolerable agreement between experimental and theoretical quantities at T_c belies a significant difference between the observed and predicted frequency dependences of the response function.

At the critical temperature, the response function observed in the vicinity of w is a three-peaked function of frequency. For moderate values of q the observed function exhibits a central ($\omega = 0$) and two, equally displaced, side peaks ascribed to collective (spin-wave) excitations. A finding of the data analysis is that a three-peaked structure persists at the smallest wave vectors, $q \sim 0.05 \text{ Å}^{-1}$, although it is obscured in the data by the resolution of the neutron spectrometer. Turning now to our predictions for the response function at T_c, figure 3(b) shows that near w there is no central peak, which one might associate with a spin diffusion process. A similar finding is reported by Wegner (1969). There is a similar, but less pronounced, discrepancy at the antiferromagnetic zone boundary. Looking at figure 4, the corresponding data reported by Tucciarone *et al* (1971a) show a well defined peak at about 4 meV (we refer to their corrected and symmeterized data with the non-magnetic background subtracted).

7. Conclusions and discussion

Dynamic spin correlations in an antiferromagnetically coupled Heisenberg magnet have been studied from the critical temperature well into the paramagnetic phase. Attention has been given to the spin–spin response function, or van Hove function, $S(k, \omega)$. This has been calculated for all vectors in the Brillouin zone. The outcome of the work is the first comprehensive study of critical and paramagnetic spin dynamics in an antiferromagnetically coupled Heisenberg magnet.

The calculations reported use the coupled-mode theory of spin dynamics. Applied to ferromagnetically coupled Heisenberg magnets, this theory is unmatched in its reliability, and range of application. Among its successes we mention correct predictions of decay rates (exponents and proportionality factors) at T_c and in the paramagnetic phase, and the influence of dipolar interactions (Frey *et al* 1989, Lovesey 1993). In consequence, we have good reasons to be confident of the value of our reported findings for an antiferromagnetically coupled magnet.

By and large, there is very good agreement, on an absolute basis, between experimental and theoretical findings for $RbMnF_3$. Quantities that have been directly compared include the dynamic critical exponent z, the temperature dependence of the decay rate at the antiferromagnetic ordering wave vector, Γ, and the half areas at various wave vectors as a function of temperature in a range from just above T_c to deep in the paramagnetic phase. However, the positive outcome of these comparisons to some extent paints a false impression, for at T_c the observed and predicted spectral lines shapes in the vicinity of the antiferromagnetic ordering wave vector are distinctly different. The observed three-peaked structure is physically appealing, since it lends itself to an intuitive and sensible interpretation in terms of diffusive and collective oscillatory processes. The absence in the predicted line shape of a central, diffusive peak, perhaps is a shortcoming of coupled-mode theory. If so, it is the only known significant shortcoming of coupled-mode theory applied to Heisenberg spin systems, and merits further experimental investigation. Bear in mind that $RbMnF_3$, by all accounts, is a near-perfect example of a Heisenberg magnet. Even the ubiquitous dipolar interactions are irrelevant variables at T_c, according to a renormalization-group analysis (Aharony 1973).

Acknowledgments

Note added in proof. An experimental investigation of RbMnF$_3$ reported by Cox *et al* (1989) gives for $T < T_c$ results that are significantly different from those of Tucciarone *et al* (1971a) made at T_c. With a small q, Cox *et al* (1989) found a much weaker central component that had an energy width comparable to the instrumental resolution. More recently, Yazaki *et al* (1994) reported data for $T = 1.2T_c$. For $q = 0.10$ and 0.40 Å^{-1} it is tolerably described by a Lorentzian function of ω. Using $\kappa = 0.17$ Å^{-1}, which is deduced from data reviewed by Als-Nielsen (1974)m, we find from (4.8) a width $\Gamma(0) = 1.04$ meV, whereas Yazaki *et al* (1994) observed $\Gamma(0) = 1.2$ meV. We note that from their data that they deduced a larger value of κ, namely, $\kappa = 0.22$ Å^{-1}. This finding is consistent with a larger value for the width since $\Gamma(0) \sim \kappa^{3/2}$.

References

Aharony A 1973 *Phys. Rev.* B **8** 3349
Als-Nielsen J 1974 *Phase Transitions and Critical Phenomena* vol 5a, ed C Domb and M S Green (London: Academic)
Bagnuls C and Joukoff-Piette C 1975 *Phys. Rev.* B **11** 1986
Collins M F 1989 *Magnetic Critical Scattering* (New York: Oxford University Press)
Cowley R A 1987 *Methods of Experimental Physics* vol 23 (Orlando, FL: Academic) part C
Cox U J, Cowley R A, Bates S and Cussen L D 1989 *J. Phys.: Condens. Matter* **1** 3031
Cuccoli A, Tognetti V and Lovesey S W 1989 *Phys. Rev.* B **39** 2619
—— 1990 *J. Phys.: Condens. Matter* **2** 3339
Frey E, Schwabl F and Thoma S 1989 *Phys. Rev.* B **40** 7199
Hubbard J 1971 *J. Phys. C: Solid State Phys.* **4** 53
Hubbard J private communication
Huber D L and Krueger D A 1970 *Phys. Rev. Lett.* **24** 111
Kawasaki K 1970 *Ann. Phys. (N.Y.)* **61** 1
Lovesey S W 1986 *Condensed Matter Physics: Dynamic Correlations (Frontiers in Physics 60)* (New York: Benjamin/Cummings)
—— 1993 *J. Phys.: Condens. Matter* **5** L251
Lovesey S W and Balcar E 1994 *J. Phys.: Condens. Matter* **6** 1253
Marshall W and Lowde R D 1968 *Rep. Prog. Phys.* B **31** 705
Privman V, Hohenberg P C and Aharony A 1990 *Phase Transitions and Critical Phenomena* vol 14, ed C Domb and J L Lebowitz (London: Academic)
Résibois P and De Leener M 1969 *Phys. Rev.* **178** 806, 819
Srivastava N, Liu J-M, Viswanath V S and Müller G A 1994 *Appl. Phys.* at press
Tucciarone A, Corliss L M and Hastings J M 1971a *J. Appl. Phys.* **42** 1378
Tucciarone A, Lau H Y, Corliss L M, Delapalme and Hastings J M 1971b *Phys. Rev.* B **4** 3206
Wegner F 1969 *Z. Phys.* **218** 260
Westhead D R, Cuccoli A, Lovesey S W and Tognetti V 1991 *J. Phys.: Condens. Matter* **3** 5235
Windsor C G and Stevenson R W H 1966 *Proc. Phys. Soc.* **87** 501
Yazaki A, Tajima K, Todate Y, Tomiyoshi S and Ikeda H 1994 *J. Phys. Soc. Japan* **63** 748